



## Non-isothermal Studies on the Thermal Decomposition of C4 Explosive Using the TG/DTA Technique

Hamid Reza POURETEDAL\*, Sajjad DAMIRI,  
Ehsan Forati GHAEMI

*Department of Applied Chemistry, Maleke-ashtar University  
of Technology, Shahin-shahr, Esfahan, I. R. Iran*

*\*E-mail: HR\_POURETEDAL@mut-es.ac.ir*

**Abstract:** The thermal behaviour of energetic materials is very important for their safe production, storage, handling and even demilitarization. In this work, the thermal behaviour and decomposition kinetics of conventional C4 plastic explosive has been studied experimentally by a non-isothermal thermogravimetric (TG)/differential thermal analysis (DTA) technique at different heating rates (2, 4, 6 and 8 °C·min<sup>-1</sup>). The kinetic triplet of activation energy, frequency factor and model of thermal decomposition of this compound has been evaluated via model-fitting and model-free methods. The results show a single thermal decomposition process for C4, with the model of integral function ( $g(\alpha)$ ) of  $[(1-\alpha)^{-1/3}-1]^2$  and differential function ( $f(\alpha)$ ) of  $[(1-\alpha)^{2/3}(3\alpha-3)/2(1-\alpha)^{1/3}-2]$ , indicating a 3-dimensional diffusion mechanism. In addition,  $E_a$  values of  $207.1 \pm 17.3$ , and  $241 \text{ kJ}\cdot\text{mol}^{-1}$ , by using the isoconversional model-free modified Kissinger-Akahira-Sunose (KAS) and the Kissinger method, respectively, were obtained for the conversion interval of 0.3-0.7. The C4 matrix shows a significant effect on the activation energy distribution of pure RDX.

**Keywords:** C4 explosive, non-isothermal, decomposition, activation energy

### 1 Introduction

The rates of the processes influencing changes in the properties of highly energetic materials during storage depends on: (i) external factors such as geometry, storage temperature, thermal insulation, and (ii) intrinsic properties of the materials such as kinetic parameters of the decomposition processes, their specific heats, and thermal conductivities [1, 2]. The kinetics and mechanisms of thermal

decomposition of explosives have considerable importance because they relate to the stability of these materials and may also be involved in the combustion processes [3, 4]. A polymer-bonded explosive, or PBX, is an explosive material in which the explosive powder is bound together in a matrix using small quantities (typically 5-10% by weight) of a synthetic polymer ("plastic"). The importance of PBX materials such as C4 is reflected in the extensive research and characterization of these materials [5-10].

The temperature dependence of the decomposition rate obtained in the test procedures for the prediction of safe storage and service life of highly energetic materials is conventionally used in the form of the Arrhenius equation [11]. Three kinetic parameters, the activation energy ( $E_a$ ), the pre-exponential factor in the Arrhenius equation ( $A$ ) and the function of the reaction progress  $f(\alpha)$ , which depend on the decomposition mechanism, are required for the prediction of the thermal stability of the materials under various applied temperature conditions. In the commonly applied computational procedures, before the calculation of the  $E$  and  $A$  values, the function  $f(\alpha)$  is often arbitrarily chosen assuming a first or zeroth order reaction. This type of assumption arbitrarily influences the determination of the kinetic parameters and significantly lowers the accuracy of the simulation of the thermal stability [12, 13].

Thermal analysis is a useful technique for the characterization of explosives. Differential scanning calorimetry (DSC) and differential thermal analysis (DTA) give information concerning thermal stability, melting, evaporation, decomposition *etc.* [14, 15]. In fact, any reaction or transformation involving absorption or release of heat can be detected with these techniques. These thermal analysis techniques have the advantage of using a small amount of sample, and rapidly often yield sufficient information for the accurate determination of the kinetic parameters of the reactions [14, 15].

In the present work, the kinetic triplet of the thermal decomposition of C4 explosive has been derived and computed by non-isothermal model-fitting and model-free methods. The Kissinger-Akahira-Sunose (KAS) method demonstrated that the differential scanning calorimetry (DSC) technique, based on the linear relation between peak temperature and heating rate, can be used to determine the thermo-kinetic parameters of a thermal decomposition (activation energy, rate constant) [16-18].

## 2 Experimental

A simultaneous thermal analysis (STA503, Bahr model) was used to record thermogravimetry (TG)/differential thermal analysis (DTA) curves of C4 explosive, containing RDX (cyclonite, 91%); dioctyladipate (DOA) plasticizer (5.3%), polyisobutylene (PIB) binder (2.1%) and motor oil (1.6%), which was synthesized in the research laboratory of Maleke-ashtar University of Technology. The TG/DTA data were collected for the temperature range 25-325 °C. The samples of the explosive, in alumina crucibles, weighed 8-10 mg. The TG/DTA data were obtained at heating rates of 2, 4, 6 and 8 °C·min<sup>-1</sup>, under a static argon atmosphere.

## 3 Results and Discussion

The TG and DTA curves of C4 explosive at four heating rates (2, 4, 6 and 8 °C·min<sup>-1</sup>) are shown in Figures 1 and 2, respectively. A single mass reduction is seen in Figure 1, indicating that C4 explosive is decomposed in a single step. The temperature at the start of decomposition were 219.0, 225.3, 229.5 and 230.8 °C at heating rates of 2, 4, 6 and 8 °C·min<sup>-1</sup>, respectively (Figure 1). A mass loss of around 90-95% was observed at all heating rates. Two endothermic peaks and one exothermic peak were observed in the DTA thermograms (see inset of Figure 2). The endothermic peaks can be attributed to heat changes that might come from its components, such as dioctyladipate (DOA) plasticizer or polyisobutylene (PIB) binder or some impurities in C4 and the melting transition of RDX explosive. It has been shown that RDX-C4 has only a single decomposition process [5-8]. The values of  $T_m$  (the peak temperature of the DTA curve) and  $T_o$  (the initial temperature at which the DTA curve deviates from the baseline of the peak) for the exothermic peaks were shifted to higher temperatures with increasing heating rate. The  $T_m$  and  $T_o$  values of the decomposition peak were observed at 220.3; 199.1, 226.5; 201.4, 231.5; 203.4 and 234.5; 205.3 °C at heating rates of 2, 4, 6 and 8 °C·min<sup>-1</sup>, respectively. Furthermore, the area under the decomposition peak increased with increasing heating rate, being 46.0, 84.9, 123.38 and 169.8  $\mu\text{V}\cdot\text{s}\cdot\text{mg}^{-1}$  at heating rates of 2, 4, 6 and 8 °C·min<sup>-1</sup>, respectively. The corresponding exothermic decomposition process of C4 explosive was observed to be at a lower temperature than that of the pure cyclic nitramine (RDX). The thermal ignition temperature of RDX and C4 are reported as 221 and 211 °C, respectively [19].

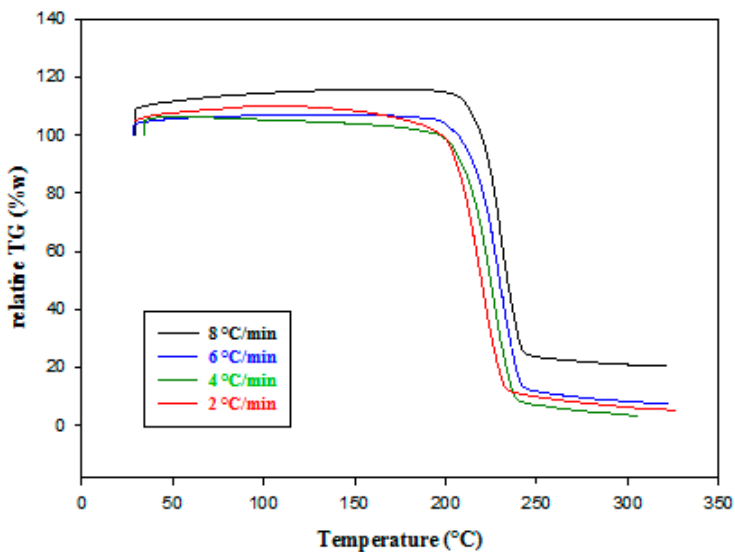


**Figure 1.** TG curves of C-4 explosive at four heating rates (2, 4, 6 and 8 °C/min).

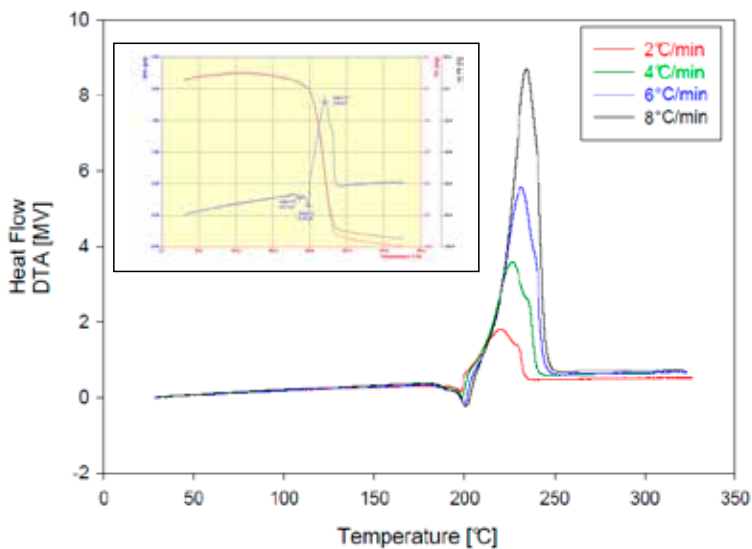


**Figure 2.** DTA curves of C-4 explosive at four heating rate (2, 4, 6 and 8 °C/min). The inset figure shows the TG/DTA curves at a heating rate of 2 °C/min.

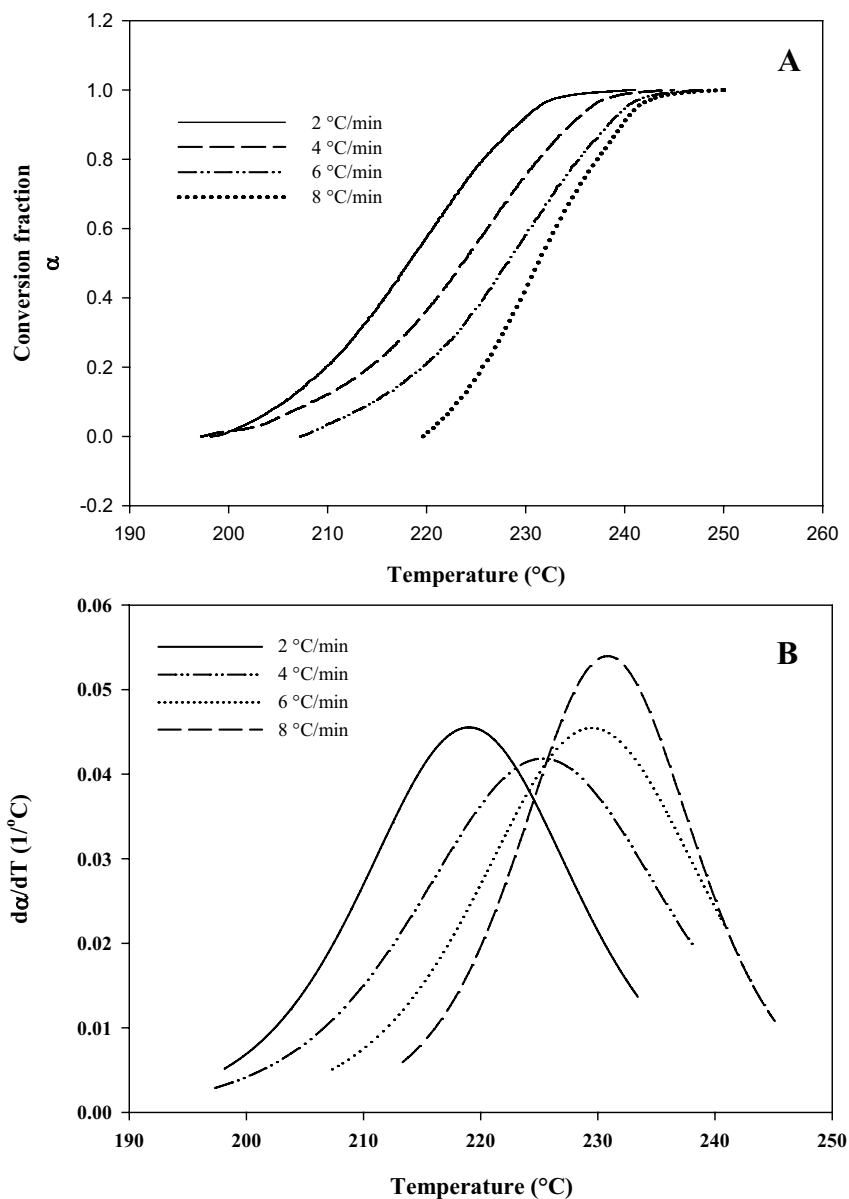


**Figure 3.** The conversion (A) and its rate curves (B) of C-4 decomposition at heating rates of 2, 4, 6, and 8  $^{\circ}\text{C}/\text{min}$ .

Here, the multiple heating rate method was employed to obtain the kinetic triplet of the apparent activation energy ( $E_a$ ), the pre-exponential constant ( $A$ )

and the mechanism of the exothermic first-stage decomposition. The most probable kinetic model functions from a single non-isothermal DTA curve of integral ( $g(\alpha)$ ) and differential ( $f(\alpha)$ ) functions were employed to predict the kinetic triplet (Equations 1 and 2).

$$\ln\left(\frac{g(\alpha)}{T - T_o}\right) = \ln(A/\beta) - \frac{E_a}{RT} \quad (1)$$

$$\ln\left(\frac{d\alpha/dT}{f(\alpha)\left[\frac{E_a(T - T_o)}{RT^2} + 1\right]}\right) = \ln(A/\beta) - \frac{E_a}{RT} \quad (2)$$

In Equations 1 and 2,  $d\alpha/dT = (1/H_o\beta)(dH/dt)$ ,  $dH/dT$  is the exothermic heat flow at time  $t$ ,  $H_o$  is the total heat effect (corresponding to the global area under the DTA curve),  $H_t$  is the reaction heat at a certain time (corresponding to the partial area under the DTA curve),  $T$  is the temperature (K) at time  $t$ ,  $\alpha$  is the conversion degree ( $\alpha = H_t/H_o$ ),  $T_o$  is the initial temperature at which the DTA curve deviates from the baseline and  $R$  is the gas constant [20-22].

The conversion-heating rate curves of C4 decomposition are presented in Figure 3, and were obtained from the experimental DTA curves. Sigmoidal models represent processes whose initial and final stages demonstrate accelerating and decelerating behaviour respectively, so that the process rate reaches its maximum at some intermediate value of the extent of conversion. These curves were obtained according to the definition of the conversion and smoothed by the Gaussian smoothing method to remove experimental noise [23, 24].

Thirty of kinetic model functions (Table 1) in integral and differential forms are used to predict the kinetic triplet [25, 26]. The values of  $E_a$  (Activation energy),  $\log A$  (preexponential constant),  $Q$  (standard mean square) and  $R^2$  (linear correlation coefficient) were obtained by the linear least-squares and iterative methods. The values of  $Q$  and  $R^2$  show that the functions of the integral function of  $[(1-\alpha)^{-1/3}-1]^2$  and of the differential function of  $[(1-\alpha)^{2/3}(3\alpha-3)/2(1-\alpha)^{1/3}-2]$  represent the most probable models for the decomposition of C4 explosive at different heating rates. The results of the selected kinetic model functions are given in Table 2. As seen, the  $E_a$  and  $A$  values obtained are 218-277 kJ·mol<sup>-1</sup> and 10<sup>14</sup>-10<sup>20</sup> s<sup>-1</sup>, respectively. Values of  $E_a$  of 197.7 ± 19.1 kJ/mol and of  $\log A$  of 18.65 ± 3.58 s<sup>-1</sup> were reported by Yan and co-workers for C4 explosive [3, 10]. Values of  $E_a$  and  $\log A$  have been reported for  $\beta$ -HMX and for  $\beta$ -HMX-C4 (227.1 kJ·mol<sup>-1</sup> and 19.70 s<sup>-1</sup>; 1023.0 ± 107.9 kJ·mol<sup>-1</sup> and 98.36 ± 12.61 s<sup>-1</sup>,

respectively) [3, 10]. The model-fitting method with various kinetic model functions is used to predict the mechanism of solid-phase reactions. The predicted function of  $g(\alpha)$  is related to 3-dimensional diffusion and shows 3-dimensional diffusion for the decomposition mechanism of C-4 explosive [27]. The function of  $f(\alpha)$  is the differential form of the  $g(\alpha)$  function.

**Table 1.** Thirty types of mechanism functions  $g(\alpha)$  and  $f(\alpha)$  used in the present analysis

No.	Symbol	Mechanism function name	$g(\alpha)$	$f(\alpha)$
1	$F_{1/3}$	One-third order	$1 - (1-\alpha)^{2/3}$	$(3/2)(1-\alpha)^{1/3}$
2	$F_{3/4}$	Three-quarters order	$1 - (1-\alpha)^{1/4}$	$2(1-\alpha)^{3/4}$
3	$F_{3/2}$	One and a half order	$(1-\alpha)^{-1/2} - 1$	$2(1-\alpha)^{3/2}$
4	$F_2$	Second order	$[1/(1-\alpha)] - 1$	$(1-\alpha)^2$
5	$F_3$	Third order	$0.5[(1-\alpha)^{-2} - 1]$	$(1-\alpha)^3$
6	$P_{3/2}$	Mampel power law	$\alpha^{3/2}$	$(2/3) \alpha^{-1/2}$
7	$P_{1/2}$	Mampel power law	$\alpha^{1/2}$	$2 \alpha^{1/2}$
8	$P_{1/3}$	Mampel power law	$\alpha^{1/3}$	$3 \alpha^{2/3}$
9	$P_{1/4}$	Mampel power law	$\alpha^{1/4}$	$4 \alpha^{3/4}$
10	$E_1$	Exponential law	$\ln \alpha$	$\alpha$
11	$A_1, F_1$	Avrami-Erofeev equation	$-\ln(1-\alpha)$	$(1-\alpha)$
12	$A_{3/2}$	Avrami-Erofeev equation	$[-\ln(1-\alpha)]^{2/3}$	$(3/2)(1-\alpha)[- \ln(1-\alpha)]^{1/3}$
13	$A_2$	Avrami-Erofeev equation	$[-\ln(1-\alpha)]^{1/2}$	$2(1-\alpha)[- \ln(1-\alpha)]^{1/2}$
14	$A_3$	Avrami-Erofeev equation	$[-\ln(1-\alpha)]^{1/3}$	$3(1-\alpha)[- \ln(1-\alpha)]^{2/3}$
15	$A_4$	Avrami-Erofeev equation	$[-\ln(1-\alpha)]^{1/4}$	$4(1-\alpha)[- \ln(1-\alpha)]^{3/4}$
16	$R_1, F_0, P_1$	Power law	$\alpha$	$(1-\alpha)^0$
17	$R_2, F_{1/2}$	Power law	$[1 - (1-\alpha)^{1/2}]$	$2(1-\alpha)^{1/2}$
18	$R_3, F_{2/3}$	Power law	$[1 - (1-\alpha)^{1/3}]$	$3(1-\alpha)^{2/3}$
19	$D_1$	Parabola low	$\alpha^2$	$1/2\alpha$
20	$D_2$	Valensi equation	$[(1-\alpha) \ln(1-\alpha)] + \alpha$	$[-\ln(1-\alpha)]^{-1}$
21	$D_3$	Jander equation	$[1 - (1-\alpha)^{1/3}]^2$	$(3/2)(1-\alpha)^{2/3} [1 - (1-\alpha)^{1/3}]^{-1}$
22	$D_4$	Ginstling-Brounstein equation	$1 - (2\alpha/3) - (1-\alpha)^{2/3}$	$(3/2)/[(1-\alpha)^{-1/3} - 1]^{-1}$
23	$D_5$	Zhuravlev, Lesokin, Tempelman equation	$[(1-\alpha)^{-1/3} - 1]^2$	$(3/2)(1-\alpha)^{4/3} [(1-\alpha)^{-1/3} - 1]^{-1}$
24	$D_6$	anti-Jander equation	$[(1+\alpha)^{1/3} - 1]^2$	$(3/2)(1+\alpha)^{2/3} [(1+\alpha)^{1/3} - 1]^{-1}$
25	$D_7$	anti-Ginstling-Brounstein equation	$1 + (2\alpha/3) - (1+\alpha)^{2/3}$	$(3/2)/[(1+\alpha)^{-1/3} - 1]^{-1}$
26	$D_8$	anti-Zhuravlev, Lesokin, Tempelman equation	$[(1+\alpha)^{-1/3} - 1]^2$	$(3/2)(1+\alpha)^{4/3} [(1+\alpha)^{-1/3} - 1]^{-1}$
27	$D1$	2-dimensional diffusion	$[1 - (1-\alpha)^{1/2}]^2$	$(1-\alpha)^{1/2} [1 - (1-\alpha)^{1/2}]^{-1}$
28	$D2$	2-dimensional diffusion	$[1 - (1-\alpha)^{1/2}]^{1/2}$	$(4)(1-\alpha)^{1/2} [1 - (1-\alpha)^{1/2}]^{1/2}$
29	$D3$	3-dimensional diffusion	$[1 - (1-\alpha)^{1/3}]^2$	$(3/2)(1-\alpha)^{2/3} [1 - (1-\alpha)^{1/3}]^{-1}$
30	$D4$	3-dimensional diffusion	$[1 - (1-\alpha)^{1/3}]^{1/2}$	$(6)(1-\alpha)^{2/3} [1 - (1-\alpha)^{1/3}]^{1/2}$

**Table 2.** The data for the probable kinetic model functions at different heating rates

Function	Heating rate [°C/min]	$E_a$ [kJ mol <sup>-1</sup> ]	log A [s <sup>-1</sup> ]	Q value	R <sup>2</sup> value
Integral (g( $\alpha$ )) [[1- $\alpha$ ] <sup>-1/3</sup> -1] <sup>2</sup>	2	277.1	20.2	0.0162	-0.9898
	4	268.9	19.7	0.0328	-0.9825
	6	253.3	17.7	0.0077	-0.9937
	8	245.3	17.0	0.0148	-0.9904
Differential (f( $\alpha$ )) [(1- $\alpha$ ) <sup>2/3</sup> (3 $\alpha$ -3)/2(1- $\alpha$ ) <sup>1/3</sup> -2]	2	231.4	15.0	0.000635	-0.9950
	4	221.0	14.6	0.0069	-0.9885
	6	236.5	15.9	0.000815	-0.9975
	8	218.8	14.2	0.000516	-0.9959

According to the recommendations of the International Confederation for Thermal Analysis and Calorimetry (ICTAC) [13], one of the proper so-called isoconversional model-free modified Kissinger-Akahira-Sunose (KAS) methods (Equation 3) could be used to obtain the kinetic triplets.

$$\ln\left(\frac{\beta_i}{T_{\alpha,i}^{1.92}}\right) = Const - 1.0008 \frac{E_\alpha}{RT_\alpha} \quad (3)$$

In this calculation of the mean activation energy, it is common practice to consider only values of  $E_\alpha$  obtained for the interval  $\alpha = 0.3-0.7$  when calculating the average value, due to the large influence of experimental conditions on the data quality of the process “tails”. During the initial and final stages of the process, the errors arising from inaccurate baseline subtraction or involvement of thermal gradients increase exponentially as the ratio between the measured signal and its background decreases. Figure 4 presents the activation energy of C4 decomposition calculated by the KAS method at different conversion values ( $\alpha$ ), with an average value of  $207.1 \pm 17.3$  kJ·mol<sup>-1</sup>. The activation energy for pure liquid and solid RDX are reported to be in the ranges of 197-199 and 213-218 kJ·mol<sup>-1</sup>, respectively [3, 5-8, 10, 19, 28].



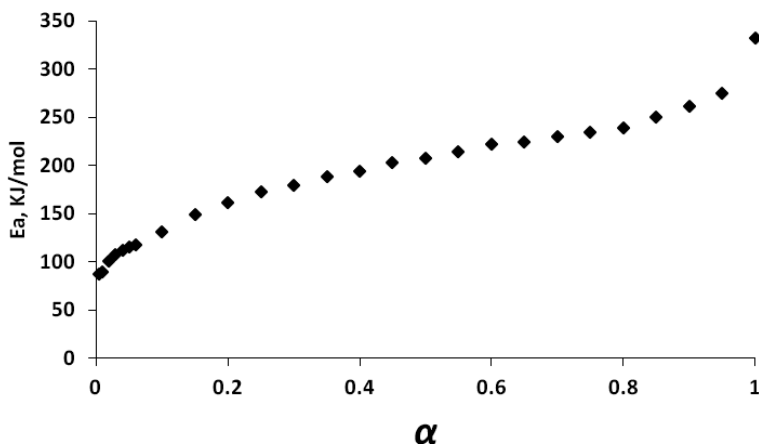


**Figure 4.** The activation energy of C-4 decomposition calculated by the Kissinger-Akahira-Sunose (KAS) method at different conversion values.

The non-isothermal, model-free method of Kissinger (Equation 4) was also used to determine the  $E_a$  value of the exothermic, first-stage decomposition reaction of C4 explosive [30]. The  $E_a$  and  $\log A$  values were obtained from the slope and intercept of the curve of  $d(\ln\beta/T_m^2)$  versus  $(1000/T_m)$ . The values of  $E_a$  and  $\log A$  obtained were  $241.8 \text{ kJ}\cdot\text{mol}^{-1}$  and  $19.3 \text{ s}^{-1}$ , respectively, with an  $R^2$  value of 0.9976 for the curve. The activation energy and pre-exponential constant obtained from the model-free method of Kissinger are within the range of the values obtained by the model-fitting method. Thus, the predicted functions by the model-fitting method could be the most probable functions for C4 decomposition.

$$\ln(\beta/T_m^2) = \ln(AR/E_a) - E_a/(RT_m) \quad (4)$$

The peak temperature ( $T_{po}$ ), corresponding to  $\beta \rightarrow 0$ , was obtained from Equation 5. The  $T_{pi}$  is the peak temperature at different heating rates of  $\beta_i$  and b, c and d are coefficients [31, 32]. The  $T_{po}$  obtained was  $213.3 \text{ }^\circ\text{C}$  by a multiple linear regression method. Finally, the critical temperature for thermal explosion ( $T_b$ ) was calculated to be  $214.9 \text{ }^\circ\text{C}$  (Equation 6), close to the reference critical temperatures of C4 and RDX ( $213$  and  $214 \text{ }^\circ\text{C}$ , respectively).  $E_o$  is the value of  $E_a$  obtained by the non-isothermal model-free method.

$$T_{pi} = T_{po} + b\beta_i + c\beta_i^2 + d\beta_i^3, \quad i = 1-4 \quad (5)$$

$$T_b = \frac{E_o - \sqrt{E_o^2 - 4E_oRT_{po}}}{2R} \quad (6)$$

## 4 Conclusions

In this paper, the thermal decomposition kinetics of C4 explosive was interpreted by using model-fitting and model-free methods. The integral function of  $[(1-\alpha)^{-1/3}-1]^2$  related to a 3-dimensional diffusion mechanism, can be used to predict the mechanism of C4 decomposition using DTA data simulation. The Kissinger-Akahira-Sunose (KAS) method offers a significant improvement in the accuracy of the  $E_a$  values and was used to determine the average value of  $E_a$ ,  $207.1 \pm 17.3 \text{ kJ}\cdot\text{mol}^{-1}$  in the range  $\alpha = 0.3-0.7$ . The calculated critical temperature of thermal explosion ( $T_b$ ) of C4,  $214.9 \text{ }^\circ\text{C}$ , was obtained according the data of the Kissinger method as a model-free method.

## Acknowledgement

We would like to thank the research committee of Malek-ashtar University of Technology (MUT) and Professor M.H. Keshavarz for supporting this work.

## 5 References

- [1] Roduit B., Borgeat Ch., Berger B., Folly P., Alonso B., Aebischer J.N., The Prediction of Thermal Stability of Self-reactive Chemicals, *J. Therm. Anal. Calorim.*, **2005**, *80*, 91-102.
- [2] Sinditskii V.P., Egorshev V.Y., Combustion Mechanism and Kinetics of Thermal Decomposition of Ammonium Chlorate and Nitrite, *Cent. Eur. J. Energ. Mater.*, **2010**, *7*, 61-67.
- [3] Yan Q.L., Zeman S., Zhao F.Q., Elbeih A., Non-isothermal Analysis of C4 Bonded Explosives Containing Different Cyclic Nitramines, *Thermochim. Acta*, **2013**, *556*, 6-12.
- [4] Singh G., Felix S.P., Soni P., Studies on Energetic Compounds. Part 31: Thermolysis and Kinetics of RDX and Some of Its Plastic Bonded Explosives, *Thermochim. Acta*, **2005**, *426*, 131-139.
- [5] Zeman S., Elbeih A., Akstein Z., Preliminary Study on Several Plastic Bonded Explosives Based on Cyclic Nitramines, *Chin. J. Energ. Mater.*, **2011**, *19*, 8-12.
- [6] Yan Q.L., Zeman S., Elbeih A., Recent Advances in Thermal Analysis and Stability Evaluation of Insensitive Plastic Bonded Explosives (PBXs), *Thermochim. Acta*, **2012**, *537*, 1-12.
- [7] Yan Q.L., Zeman S., Svoboda R., Elbeih A., Málek J., The Effect of Crystal Structure

- on the Thermal Initiation of CL-20 and Its C4 Bonded Explosives (II): Models for Overlapped Reactions and Thermal Stability, *J. Therm. Anal. Calorim.*, **2013**, *112*, 837-849.
- [8] Yan Q.L., Zeman S., Elbeih A., Song Z.W., Málek J., The Effect of Crystal Structure on the Thermal Reactivity of CL-20 and Its C4 Bonded Explosives (I): Thermodynamic Properties and Decomposition Kinetics, *J. Therm. Anal. Calorim.*, **2013**, *112*, 823-836.
- [9] Zeman S., Elbeih A., Yan Q.L., Notes on the Use of the Vacuum Stability Test in the Study of Initiation Reactivity of Attractive Cyclic Nitramines in the C4 Matrix, *J. Therm. Anal. Calorim.*, **2013**, *112*, 1433-1437.
- [10] Yan Q.L., Zeman S., Elbeih A., Thermal Behaviour and Decomposition Kinetics of Viton A Bonded Explosives Containing Attractive Cyclic Nitramines, *Thermochim. Acta*, **2013**, *562*, 56-64.
- [11] Sbirrazzuoli N., Vincent L., Mija A., Guigo N., Integral, Differential and Advanced Isoconversional Methods Complex Mechanisms and Isothermal Predicted Conversion-time Curves, *Chemometr. Intell. Lab.*, **2009**, *96*, 219-226.
- [12] Moukhina E., Determination of Kinetic Mechanisms for Reactions Measured with Thermoanalytical Instruments, *J. Therm. Anal. Calorim.*; DOI 10.1007/s10973-012-2406-3.
- [13] Vyazovkin S., Burnham A.K., Criado J.M., Pérez-Maqueda L.A., Popescu C., Sbirrazzuoli N., ICTAC Kinetics Committee Recommendations for Performing Kinetic Computations on Thermal Analysis Data, *Thermochim. Acta*, **2011**, *520*, 1-19.
- [14] Hemmilä M.O., Use of Thermal Analysis in Compatibility Testing of 2, 4, 6-Trinitrotoluene, *J. Therm. Anal.*, **1982**, *25*, 135-138.
- [15] Chen G., Lee C., Kuo Y.L., Yen Y.W., A DSC Study on the Kinetics of Disproportionation Reaction of (hfac) Cu(COD), *Thermochim. Acta*, **2007**, *456*, 89-93.
- [16] Fengqi Z., Rongzu H., Jirong S., Hongxu G., Kinetics of the Exothermic Decomposition of 1-Nitro-3-( $\beta,\beta,\beta$ -trinitroethyl)-4,5-dinitroiminoimidazolidine-2-one, *Russ. J. Phys. Chem.*, **2006**, *80*, 1034-1036.
- [17] Svoboda R., Málek J., Interpretation of Crystallization Kinetics Results Provided by DSC, *Thermochim. Acta*, **2011**, *526*, 237-251.
- [18] Málek J., The Kinetic Analysis of Non-isothermal Data, *Thermochim. Acta*, **1992**, *200*, 257-269.
- [19] Akhavan J., *The Chemistry of Explosives*, 3rd ed., Roy. Soc. Chem. Publishing, UK, **2011**, pp. 49-113.
- [20] Rongzu H., Desuo Y., Fengqi Z., Pei C., Yang L., Sanping C., Hongan Z., Jirong S., Shengli G., Qizhen S., Kinetics and Mechanism of Exothermic First-stage Decomposition Reaction for 2,6-Dinitro-4,8-bis(2,2,2-trinitroethyl)-2,4,6,8-tetraazabicyclo[3.3.1]nonane-3,7-dione, *Chem. Res. Chinese*, **2004**, *20*, 821-825.
- [21] Khawam A., Flanagan D.R., Solid-state Kinetic Models: Basics and Mathematical Fundamentals, *J. Phys. Chem. B*, **2006**, *110*, 17315-17328.

- [22] Chen H., Liu N., Application of Non-Arrhenius Equations in Interpreting Calcium Carbonate Decomposition Kinetics: Revisited, *J. Am. Ceram. Soc.*, **2010**, *93*, 548-553.
- [23] Sbirrazzuoli N., Vincent L., Mija A., Guigo N., Integral, Differential and Advanced Isoconversional Methods Complex Mechanisms and Isothermal Predicted Conversion-time Curves, *Chemometr. Intell. Lab.*, **2009**, *96*, 219-226.
- [24] Segal E., Rate Equations of Solid State Reactions. Euclidean and Fractal Models, *Revue Roumaine de Chimie*, **2012**, *57*, 491-493.
- [25] Burnham A., Computational Aspects of Kinetic Analysis. Part D: The ICTAC Kinetics Project – Multi-thermal-history Model-model-fitting Methods and Their Relation to Isoconversional Methods, *Thermochim. Acta*, **2000**, *355*, 165-70.
- [26] Khawam A., Flanagan D.R., Solid-State Kinetic Models: Basics and Mathematical Fundamentals, *J. Phys. Chem. B*, **2006**, *110*, 17315-17328.
- [27] Opfermann J., Kinetic Analysis Using Multivariate Non-linear Regression – I. Basic Concepts, *J. Therm. Anal. Calorim.*, **2000**, *60*, 641-658.
- [28] Long G.T., Vyazovkin S., Brems B.A., Wight C.A., Competitive Vaporization and Decomposition of Liquid RDX, *Phys. Chem. J.*, **2000**, *104*, 2570-2574.
- [29] Zhu Y.L., Huang H., Ren H., Jiao Q.J., Influence of Aluminum Particle Size on Thermal Decomposition of RDX, *J. Energ. Mater.*, **2013**, *31*, 178-191.
- [30] Laidler K.J., The Development of the Arrhenius Equation, *J. Chem. Educ.*, **1984**, *61*, 494-498.
- [31] Zhao F.Q., Gao H.X., Hu R.Z., Lu G.E., Jiang J.Y., A Study of Estimating the Safe Storage Life, Self-accelerating Decomposition Temperature and Critical Temperature of Thermal Explosion of Double-base Propellant Using Isothermal and Non-isothermal Decomposition Behaviours, *Chinese Chem. Lett.*, **2006**, *17*, 667-670.
- [32] Tarver C.M., Tran T.D., Thermal Decomposition Models for HMX-based Plastic Bonded Explosives, *Combust. Flame*, **2004**, *137*, 50-62.